JOURNAL OF MATERIALS SCIENCE 21 (1986) 3015–3018

High temperature creep in polycrystalline AlN–SiC ceramics

Z. C. JOU, S. Y. KUO, A. V. VIRKAR
Department of Materials Science and Engineering, University of Utah, Salt Lake City, Utah 84112, USA

Polycrystalline dense ceramic specimens containing 75 mol % AlN–25 mol % SiC and 60 mol % AlN–40 mol % SiC were subjected to creep deformation in bending at elevated temperatures. Over the range of temperatures and stresses investigated, the creep rate was found to vary linearly with stress indicative of diffusional creep. Creep was found to be thermally activated with activation energy in the range from 175 kcal mol^{-1} to 219 kcal mol^{-1}. Electron microscopic observation indicated that crack like cavities formed near the tensile surfaces during creep.

1. Introduction

Silicon carbide (SiC) and aluminiun nitride (AlN) are two of the important structural ceramics for application at low as well as at high temperatures. There have been numerous studies on the fabrication and the characterization of SiC. By contrast there have been only a few studies on AlN. Sakai [1, 2] determined the flexural strength of AlN with various amounts of Al_2O_3 added to it. Strengths as high as 500 MPa were observed at 1500° C and the fracture morphology was typical of brittle fracture. For application at elevated temperatures, resistance to creep is an important consideration. Several researchers [3–11] have studied the creep of SiC. Creep was found to be thermally activated although the value of the activation energy for creep reported by investigators ranged between 35 and 212 kcal mol^{-1}. Furthermore, stress exponents were found to be as low as 1.0, indicative of diffusional creep, to as high as 5.7 suggestive of creep controlled by dislocation climb.

AlN and the 2H polymorph of SiC are known to form an extensive solid solution [12–14]. Furthermore, at low temperatures, phase separation into two solid solutions of the 2H type was shown to occur [13]. It is anticipated that AlN–SiC solid solutions or two phase alloys will be an important class of structural ceramics since property engineering is possible by an appropriate choice of compositions and thermal treatments [15]. Preliminary work [15] in fact has shown that the creep rate of SiC + 35 wt % AlN is comparable to that of essentially pure SiC at 1450° C. The potential of AlN–SiC ceramics for high temperature applications can only be assessed through elevated temperature testing as a function of composition. The objective of the present work was to evaluate high temperature deformation characteristics of AlN–SiC ceramics with AlN as the major constituent.

AlN–SiC ceramics of two different compositions: 75 mol % AlN–25 mol % SiC and 60 mol % AlN–40 mol % SiC were fabricated by hot pressing mixtures of AlN and SiC powders. Bar-shaped samples were subjected to creep deformation in four-point bending in air. Rate of deformation was measured as a function of stress applied and temperature. Transmission electron microscopy (TEM) and scanning electron microscopy (SEM) were the principal characterization tools employed.

2. Experimental procedure

2.1. Sample preparation

Disc-shaped specimens were fabricated by hot pressing a mixture of AlN (H. Starck Company, West Germany) and α-SiC (A-10, H. Starck Company, West Germany) in graphite dies in an atmosphere of nitrogen. Pertinent information on the starting powder, as provided by the supplier, is given in Table I. Samples containing 75 mol % AlN–25 mol % SiC (hereafter abbreviated 75/25) were hot pressed at a temperature of 2185° C for 0.5 h under a pressure of 30 MPa. Samples containing 60 mol % AlN–40 mol % SiC (herafter abbreviated 60/40) were hot pressed at 2260° C for 1 h under a pressure of 30 MPa. Samples were characterized with regards to the phase content (using X-ray diffraction), microsctructre and density. Rectangular beam-shaped specimens of dimensions 0.2 cm × 0.5 cm × 3.0 cm were machined out of the hot pressed billets. The samples were lapped on a 30 μm diamond wheel. The dimensions of the samples were controlled to within ± 0.001 cm.

2.2. Creep testing

Samples were subjected to creep deformation in four-point bending in air. The apparatus for creep testing, designed and built in the laboratory, consists of an electrical furnace with molybdenum disilicide heating elements. The loading fixture consists of a thick walled alumina tube with grooves in which sapphire rods are

TABLE I

Material	Surface area ($m^2 g^{-1}$)	Impurities
Starck–α-SiC	13–17	O: 0.4%, free C: 0.2%
Starck AlN	2–4	O: 1.0 to 1.5% C: 0.05%, Fe: 0.1%

0022–2461/86 $03.00 + .12

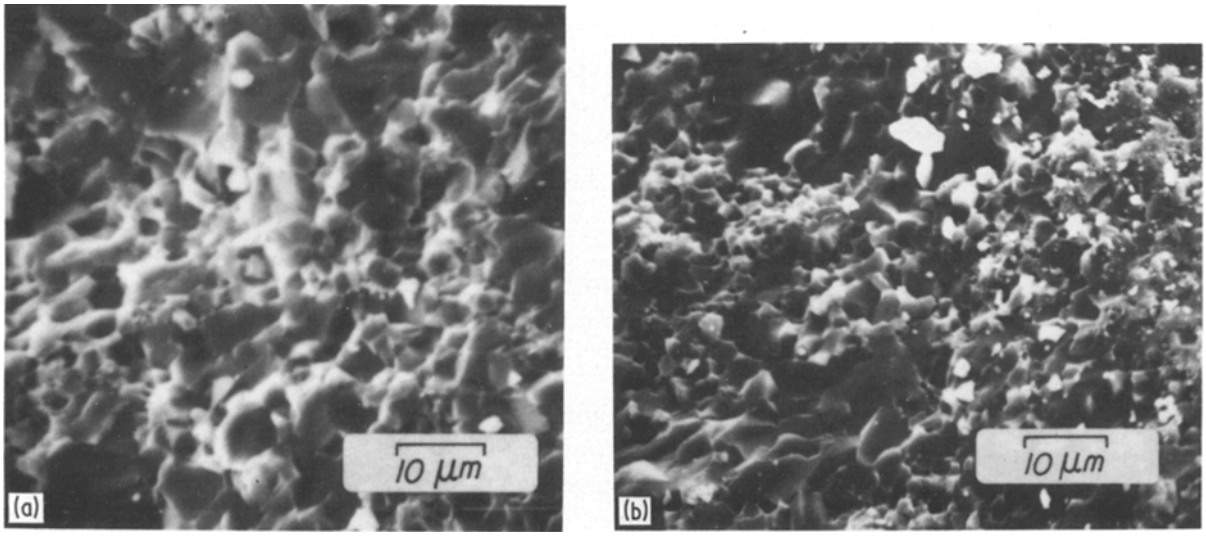

Figure 1 An SEM fractograph of (a) 75/25 and (b) 60/40 specimen showing equiaxed microstructure with some exaggerated grain growth.

housed. A specimen is supported on the sapphire rods and load, in the four-point geometry, is applied. The deflection is measured using a linear voltage differential transformer (LVDT) and is recorded continuously on a strip chart recorder. The applied load and the measured deflection rate are converted into the stress and the strain rate respectively, using the appropriate geometrical relationships [16]. During the creep experiment, surface regions of the specimens were oxidized. The maximum total oxide thickness, however, was less than 6% of the specimen thickness. Appropriate correction was made to take this into account.

2.3. Electron microscopy

Some of the samples were deliberately fractured at room temperature and were subsequently examined under SEM for the approximate estimation of grain size. Scanning electron fractography was used for this purpose because it was found difficult to reveal the microstructure by chemically etching polished surfaces.

One of the samples of 75/25 composition subjected to creep deformation was mechanically thinned down to about 30 μm and was ion milled to perforation for examination in a scanning transmission electron microscope* (STEM). TEM foils from both the tensile and the compressive regions of the creep sample were examined.

3. Results

The density of the hot pressed specimens was near theoretical. For 75/25 it was 3.218 g cm^{-3} (99.1% of the theoretical density) and for 60/40 it was 3.227 g cm^{-3} (99.6% of the theoretical density). X-ray diffraction indicated 2H as the predominant crystal type with traces of other polytypes as well. Difficulty was encountered in chemical etching of the specimens to reveal the microstructure. In order to gain some information about the microstructure, some of the specimens were fractured and fracture surfaces were examined under SEM. Fig. 1 shows SEM fractographs of the 75/25 and the 60/40 specimens. Fracture is predominantly intergranular in both the specimens. Approximate grain size measurement indicates $d \sim 8\,\mu$m in 75/25 and $d \sim 5\,\mu$m in 60/40. Grain size distribution is seen to be bimodal with some rather large grains. Although the microstructure is seen to be equiaxed, there is some spatial variation in the grain size which probably results from chemical inhomogenities.

The measured deflection at the loading pins was converted into strain in the outer fibres using the following equation [16]

$$\varepsilon = \frac{2h\,(N + 2)\delta}{(L - l)[L + l(N + 1)]} \qquad (1)$$

where h is the specimen thickness, δ is the deflection at the loading pins, L and l are the distances between the outer and the inner supports respectively and N is the stress exponent of creep rate.

Log $\dot{\varepsilon}$ is plotted against $1/T$ where T is in Kelvin, in Fig. 2 for both 75/25 and 60/40 specimens. The data plotted in Fig. 2 correspond to the steady state. The steady state was generally established within 2 to 3 days after the application of stress at a given temperature. In both types of specimens, creep was found to be thermally activated. The activation energy for 60/40 samples was between 175 and 176 kcal mol^{-1} for the data on the two samples shown in Fig. 2. For the 75/25 specimen, the activation energy was found to be 219 kcal mol^{-1}. The highest creep rate measured at 1723 K for the 60/40 specimens was 2.71×10^{-8} sec^{-1} and for 75/25 specimen it was 3.08×10^{-8} sec^{-1}. Since the creep testing was conducted in air, an oxide film was formed during creep testing. The oxide thickness was typically 30 to 40 μm which is quite small in comparison with the specimen thickness of 0.2 cm or 2000 μm. It was assumed that oxide layer is softer than the ceramic i.e. it creeps faster. Thus, the strain and the stress calculations were made by subtracting the oxide thickness. Oxidation kinetics studies [17] permitted the estimation of the instantaneous oxide film thickness. Since the film thickness was much smaller than the sample thickness, however, the correction was negligible.

*JEM 200 CX, Japan Electronic Optics Laboratory, Tokyo.

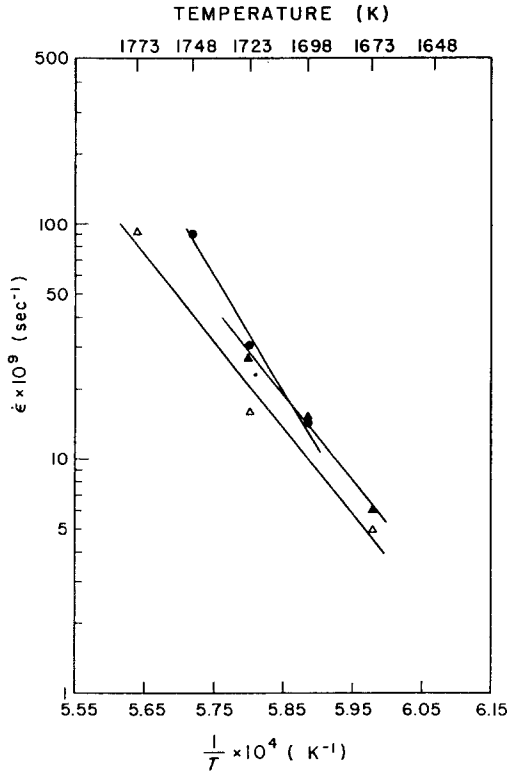

Figure 2 Plots of log $\dot{\epsilon}$ against $1/T$ for 75/25 and 60/40 specimens. Arrhenus plot for creep of AlN–SiC. Stress 81 MPa. 75/25 (●) E_a = 219 kcal mol^{-1}; 60/40 (△) E_a = 176 kcal mol^{-1}; (▲) E_a = 175 kcal mol^{-1}.

In order to determine the stress dependence of the steady state creep rate, stress was varied between 50 and 150 MPa. At 1673 K, for 75/25 the creep rate was found to be nearly linearly proportional to the stress (stress exponent, N, in $\dot{\epsilon} \propto \sigma^N$ was found to be 1.18) and for 60/40 at 1698 K N was found to be 1.02 (see Fig. 3). Creep rate for 75/25 specimens was about the same as for 60/40 specimens over the range of temperatures studied.

Investigation under STEM revealed the presence of substantial dislocation density. Fig. 4 shows the dislocations observed in the tensile regions of the samples. A significant dislocation density was also observed in

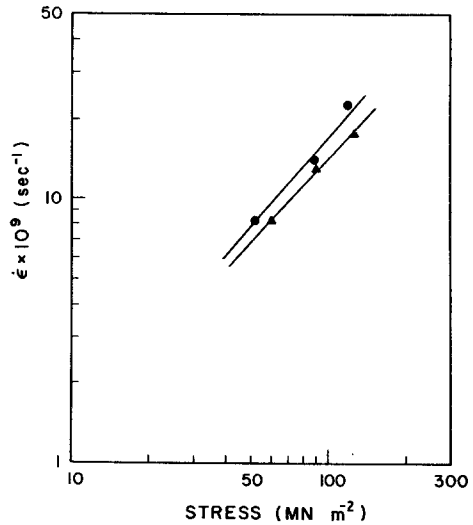

Figure 3 Plots of log $\dot{\epsilon}$ against log σ for 75/25 and 60/40 specimens. For 75/25 (●) N = 1.18 at 1673 K while for 60/40 (▲) N = 1.02 at 1698 K.

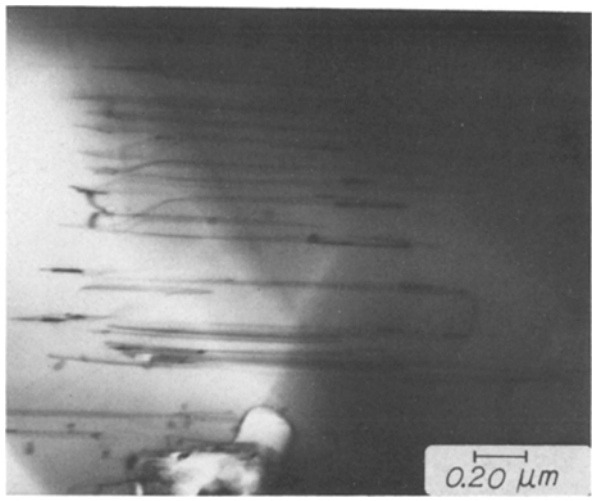

Figure 4 A transmission electron micrograph of a 75/25 specimen (tension side) exhibiting dislocations.

the hot pressed specimens as well. Carter *et al.* [9] also reported a high dislocation density in reaction bonded SiC. The 75/25 specimens, which were examined in some detail, showed formation of cavities at the three grain junctions as well as the formation of crack-like cavities along the grain boundaries (see Fig. 5). The crack-like cavities were observed only on foils made from the tensile side of the specimens but not from the compressive side.

4. Discussion

Temperature dependence of the creep rate in both 75/25 and 60/40 specimens indicates a thermally activated process, as generally to be expected. For 75/25, the activation energy is 219 kcal mol^{-1} while for 60/40 it is in the range from 175 to 176 kcal mol^{-1}. No data were available in the literature on AlN–SiC ceramics of these compositions. However, for pure AlN, the activation energy for sintering [18] kinetics is known to be as high as about 130 kcal mol^{-1}. Activation energy for creep in SiC published by numerous authors [3–11] ranged between 35 and 212 kcal mol^{-1}. Activation energies measured in the present work are in the general range of these values.

Stress dependence of the creep rate showed that the creep rate varies linearly with the stress indicative of diffusional creep. In pure SiC, stress exponent has been found to vary between one and 5.7 [9] suggesting diffusional and dislocation climb controlled creep respectively as the dominating mechanisms. In the present work, dominating creep mechanisms appear to be diffusional. It is not known at the present time whether volume diffusion or grain boundary diffusion is the dominant mode of mass transport. If grain boundary diffusion is the dominant mode, $\dot{\epsilon} \propto d^{-3}$, while for volume diffusion as the dominant mechanism the expected dependency is given by $\dot{\epsilon} \propto d^{-2}$. Although the grain structure is equiaxed, there is some exaggerated grain growth probably resulting from chemial inhomogeneities. The fact that there was an increase in dislocation density in the samples (75/25) after subjecting to creep suggests that dislocation glide or glide/climb also contributes to creep but is not the dominant mechanism of strain accumulation.

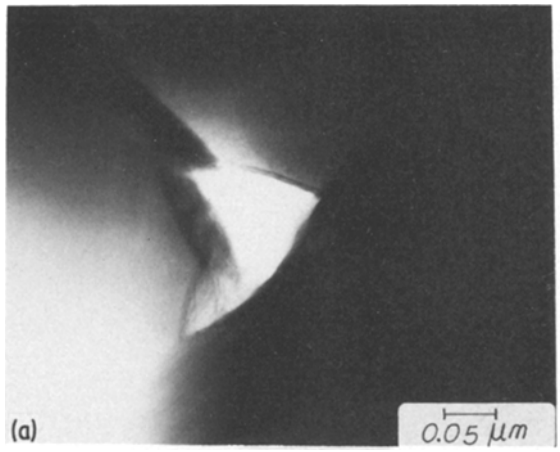

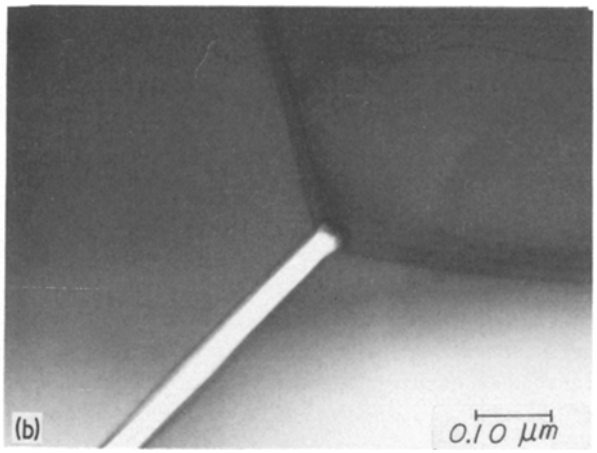

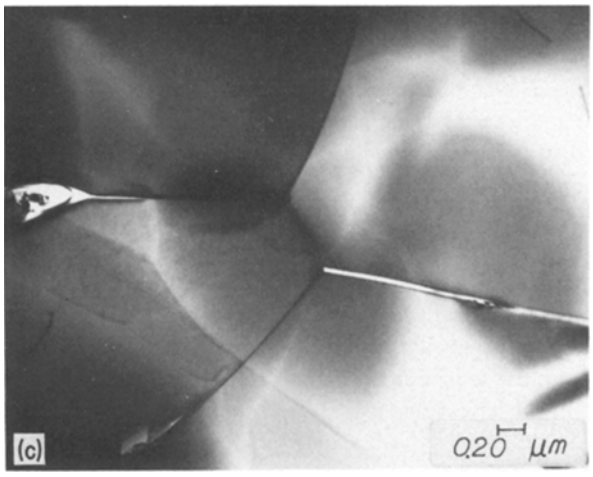

Figure 5 Transmission electron micrographs of cavities formed in 75/25 specimens. (a) A cavity at a three grain junction (b) crack-like cavities at grain boundaries (c) a crack-like cavity along a grain boundary.

If it is assumed that grain boundary diffusion is the dominant mode of deformation, then the appropriate creep equation is given by [19]

$$\dot{\varepsilon} = \frac{44\Omega_v \sigma D_b \lambda}{k_B T d^3} \quad (2)$$

where Ω_v is the molecular volume, d is the grain size, D_b is the pertinent grain boundary diffusivity, λ is the grain boundary thickness, k_B is Boltzmann's constant and T is the temperature in Kelvin. Assuming $\Omega_v = 3 \times 10^{-29}\,m^3$, $d = 5 \times 10^{-6}\,m$, at 1673 K with $\sigma = 80\,MPa$, $\dot{\varepsilon} = 6 \times 10^{-9}\,sec^{-1}$, $D_b\lambda$ for 40% AlN–60% SiC is given by $D_b\lambda \sim 1.64 \times 10^{-25}\,m^3\,sec^{-1}$. Assuming $\lambda = 10\,Å = 10^{-9}\,m$, the grain boundary diffusivity, D_b, is given by

$$D_b = 1.64 \times 10^{-16}\,m^2\,sec^{-1} \text{ or}$$

$$1.64 \times 10^{-12}\,cm^2\,sec^{-1}.$$

There are no data available regarding grain boundary diffusivity in AlN–SiC. However, the above value appears reasonable. Further work with specimens of varying grain size would be required to confirm mechanisms of deformation.

Formation of crack like cavities along the grain boundaries, as shown in Fig. 5, suggests that the accommodation was not strictly diffusional. These crack-like cavities were observed predominantly on the tensile side of the specimen. Further, they appear to occur in a specific direction, probably orthogonal to the applied stress. Cavities at the three grain junction were also observed in numerous cases. The formation of crack-like cavities may be a precursor to extended subcritical crack growth as observed by McHenry and Tressler [20] in SiC. It is anticipated that coalescence of such microcracks would occur in the tertiary stage of creep leading to final rupture.

In conclusion, creep in AlN–SiC is thermally activated and the dominant mechanism is diffusional.

Acknowledgement

This work was supported by the US Department of Energy under Contract Number DEACO284ER45049.

References

1. T. SAKAI, *J. Amer. Ceram. Soc.* **61** (1978) 460.
2. *Idem, ibid.* **64** (1981) 135.
3. J. C. V. RUMSEY and A. L. ROBERTS, *Proc. Brit. Ceram. Soc.* **2** (1967) 233.
4. P. MARSHALL and R. B. JONES, *Powder Metall.* **12** (1967) 193.
5. V. KRISHNAMACHARI and M. R. NOTIS, *Mater. Sci. Eng.* **27** (1977) 83.
6. D. C. LARSEN and G. C. WALTHER, AFML Report. No. IITRI-D6114-ITR-24 (Illinois Institute of Technology Research Institute, 1977).
7. *Idem,* Report No. 11, Contract F33615-79-C-5100 (Illinois Institute of Technology Research Institute, 1981).
8. M. S. SELTZER, AFML-TR-76-97, (1976).
9. C. H. CARTER Jr, R. F. DAVIS and J. BENTLEY, *J. Amer. Ceram. Soc.* **67** (1984) 409.
10. *Idem, ibid.* **67** (1984) 732.
11. H. TANAKA and Y. INOMATA, *Yogyo-Kyokai-Shi* **93** (1985) 11.
12. I. B. CUTLER, P. D. MILLER, W. RAFANIELLO, H. K. PARK, D. P. THOMPSON and K. H. JACK, *Nature* **275** (1975) 434.
13. W. RAFANIELLO, M. R. PLICHTA and A. V. VIRKAR, *J. Amer. Ceram. Soc.* **66** (1983) 272.
14. R. RUH and A. ZANGVIL, *ibid.* **65** (1982) 260.
15. W. RAFANIELLO, K. CHO and A. V. VIRKAR, *J. Mater. Sci.* **16** (1981) 3479.
16. G. W. HOLLENBERG, G. R. TERWILLIGER and R. S. GORDON, *J. Amer. Ceram. Soc.* **54** (1971) 196.
17. Z. C. JOU and A. V. VIRKAR, unpublished work (1985).
18. K. KOMEYA and H. INOUE, *J. Mater. Sci.* **4** (1969) 1045.
19. R. L. COBLE, *J. Appl. Phys.* **34** (1963) 1679.
20. K. D. McHENRY and R. E. TRESSLER, *J. Amer. Ceram. Soc.* **64** (1980) 152.

Received 9 September
and accepted 11 October 1985